Anonymous Referee #1

This paper describes the application of a coupled pedogenic-geomorphic model to a semi-arid field site in Israel. The authors demonstrate that a model that combines transport by diffusive hillslope processes (creep and bioturbation) with transport by overland and rill flow does a better job at reproducing observed soil depths than a model that contains just one of these transport types. The paper concludes that different parts of the hillslopes tend to be dominated by one of the two transport mechanisms: diffusion at the top and fluvial at the bottom.

First of all we would like to thank the referee for this very thorough review. Below we provide a point-by-point response to the reviewer's comments.

That a model that includes both fluvial and diffusive processes works better than one with just diffusion or just fluvial processes does not strike me as a significant conclusion. I don't understand why the authors would run simulations with diffusive processes only or fluvial processes only, given that all landscapes clearly have both of these transport types occurring. The reason why is clearly and repeatedly described and discussed. In a nutshell: the relationship between these transport types are well explored in bedrock-weathering dominated but not in aeolian soilscapes. Moreover, we investigate the effects of temporal variability in external drivers (i.e. climatic/anthropogenic scenarios, a key aspect of the overarching research) that seems to, based on our literature review for this region, differ for the two transport mechanisms. We therefore need to isolate each mechanism in order to identify their specific spatial and temporal dynamics. The conclusion of this study is NOT that both transport mechanisms are in play but rather a suite of insights on their specific dynamics and interactions.

Model concerns:

Equation 1: Nothing like equation 1 appears in Engelund and Hansen (1968). In sediment transport the flux usually goes as the square root of the excess density, not the square of excess density We disagree with this statement (see page 48 in Engelund and Hansen (1968)) but acknowledge that we should have been more specific. This equation was based on the TOPOG model sediment transport calculations which used the Engelund and Hansen (1968) equation (http://www-data.wron.csiro.au/topog/user/contents/frame1.0.html). This is now clearly outlined in the revised manuscript.

(which is usually s-1, not 1-s as shown here). True, this was a typo but make no difference to the result as the expression is squared and s is constant.

The assumption that sediment flux is linear with water discharge (i.e. n_1 = 1) is inconsistent with all sediment transport formula in the literature. The n1 and n2 values are in line with the TOPOG values.

The publication year is 1967, not 1968, and Engelund's name is misspelled. Corrected.

Equation 2: Why do the authors assume n_4 = 0.1? No reason is given. This is an extremely low scaling relationship between discharge and area. It is explained: *"In Cohen et al. (2010 and 2015) the relationship between contributing area and runoff discharge was assumed to be linear (n4=1). This assumption could not be justified in our field-site as Yair and Kossovsky (2002) showed that runoff generation in this region does not increase linearly downslope. We therefore use n4=0.1 in this study."*

Routing: D8 routing is inappropriate for hillslopes. The authors need to use a multiple flow direction algorithm. As the authors state, the unrealistic "striping" of the model output along 45 deg angles is a result of the routing algorithm. This limitation is discussed in previous papers. One of the main advances in the mARM model is its computational efficiency which allowed, for the first time, for such explicit and long-term simulations at landscape scales. Recent advances with this framework and similar models may now allow us to consider more runtime-expensive routing algorithms. This is a topic for a whole different paper.

However, it is very strange that the striping occurs only for the diffusive simulation, which does not involve routing at all as far as I can determine from the text. Diffusion absolutely involved routing, how else does the model transport the sediment down the slope? It is, however, not directly affected by contributing area and so there is no downstream scaling and the stripping occurs along the hillslope in places where the flow directions are parallel.

Equations 3&4: This does not look like hillslope diffusion. This stem from our attempt to simplify a complex 5D (x, y, z, t and PSD) algorithm in a couple of equations. As we describe, this is a novel equation and is described and explored in more details in Cohen et al. (2015). It is now better explained in the revised manuscript.

The authors have assumed that the colluvial transport rate increases as the 0.1 power of slope, not the usual linear formulation (or the nonlinear formulation of Bucknam and Andrews, Roering et al., etc.). No results of the calibration used to obtain beta = 0.1 is provided. In Cohen et al. (2015) we used a linear relationship (b=1) and have conducted an extensive parametric study for beta for this study. See the relationship between slope and diffusion rate for beta = 0.1 and 1 in the plots bellow. The fact that beta differs from 1 to such an extent in this field-site is actually very interesting! We propose that it could be another aeolian-driven affect (fine PSD, absence of armoring etc.) or is due to the relatively steep and concave down shape of the hillslopes in this site (so site-specific). This is now explained (in the model description) and discussed (in the discussion section) in the revised manuscript.

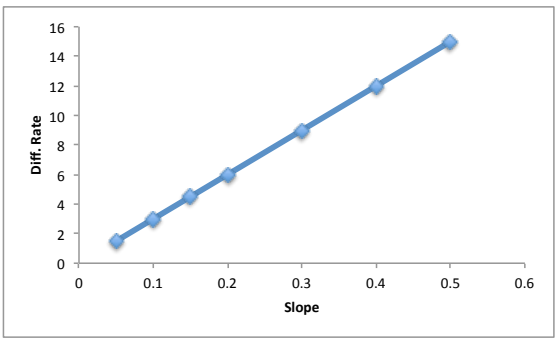

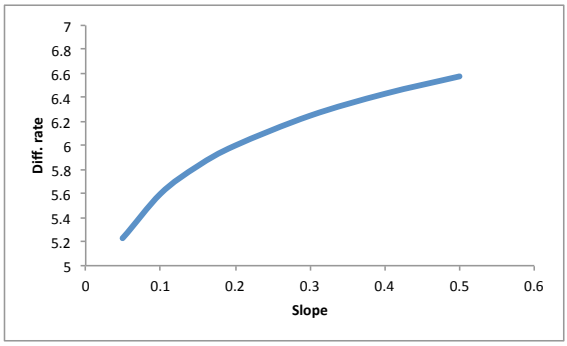

The units of the various parameters are very hard to keep track of and clearly wrong in some cases. D_s should not have units of time because the time step is included in equation 4 (D_s should have units of m, not m/yr). Not true! Equation 4 doesn't have a time step parameter, it describes changes in D (m/s) down the profile. In practice it makes not difference.

What is k? What are its units and its value? "…k is the surface diffusivity (m)" its values are described in section 2.4. We changed k to D_o to distinguish it from k_a.

Equation 5: The reader is referred to Minasny and McBratney (2006), which is not in the reference list. Corrected

When I tracked down Minasny and McBratney (2006) I found a rather different equation (their equation (4)). Equation (5) is dimensionally incorrect. It is wrong to have the steady state weathering rate appear inside the exponential – the argument of any exponential should be unitless. The equation was indeed (as stated) modified, the Po parameter was moved to allow for an above-zero watering rate at the surface while depth rates down the soil profile asymptote to zero. Cohen et al. (2010) focused on the model weathering equations and algorithm. We can see how the description of the model weathering calculations is confusing and misrepresentative. This stems, again, from our attempt to simplify a complex algorithm into one equation with time-varying parameter. The full algorithm includes compiling a transition matrix which control the transition of PSD in each particle size class to smaller class(s) in each soil-profile layer. The algorithm was described at length in Cohen et al. (2009 and 2010). The depth-varying weathering rate equation in the model (see the actual model FORTRAN function below) is not directly used to calculate weathering rate, rather the relative (normalized) change in weathering down the profile. As part of the revised model description we removed the section describing the weathering calculations as it does not include parameters that are modified in the simulation scenarios we analyzed in this paper.

```
!######################################################################
! A function to calculate the decline in weathering rate as a function of depth
! It return the WeatheringAlpha which is different for every layer
! The exponential function is taken from Minasny & McBratney (2006)
! de/dt=Po{Exp(-k1h)-Exp(-k2h)}+Pa ;
! Their original values are: Po-potential WR=0.25; k1=4; k2=6; Pa- steady state WR=0.005
! The function was changed in version 4.5.1 to account to close to zero weathering in
lower layers
!######################################################################
    REAL*8 Function DepthWeatheringAlpha(WeatherAlpha,i,LayerDepth)
    IMPLICIT NONE
```

```
    Integer i
    Real*8 WeatherAlpha, LayerDepth, Ratio, Depth
    If (i==1) Then
    Depth=0.5
    Else
    Depth=(i-1)*LayerDepth-(LayerDepth/2)
    End If
    Depth=Depth/100 !convert to meters
    Ratio=(0.25*((EXP(-4*Depth+0.02))-(EXP(-6*Depth))+0))/0.04 !We divide by 0.04 to
normalize it
    DepthWeatheringAlpha = WeatherAlpha*Ratio
    Return
    End Function DepthWeatheringAlpha
```

Why are delta_1 and delta_2 equal to 4 and 6? What are the units? If they are meters these are very large values (i.e. they imply that weathering rates fall off by a factor of e only once the soil is at least 4 m thick. This is a very thick soil). Following on the comment above, the model algorithm uses the Minasny and McBratney (2006) equation to get the relative change in weathering rate down the soil profile. These variables therefor control the shape rather then the actual weathering rate. Their values were based on Minasny and McBratney (2006) to maintain the relative change (i.e. shape of the hump function) and so in reality they are unitless.

How the equations are combined is not clear. There must be some conservation equation being used in the model (e.g. erosion rate is related to the divergence of sediment flux), but this is not shown. I did find something like a conservation equation in Cohen et al. (2015), but that equation is dimensionally incorrect (the erosion rate (which has units of L/T) is equated with sediment flux, which has units of L^2/T). Again, as we showed above, there is no dimensionality issue with the actual implementation of the equation. As we stated at the start of section 2.2 the full description of the model architecture is provided in Cohen et al. (2009 and 2010). The model description in this paper is limited to the equations "that include the parameters that are modified by the simulation scenarios we analysed here." A short description of the model architecture was added to the revised manuscript.

Fluvial erosion from hillslopes is generally modeled as a 2-step process: 1) rainsplash disturbance of soil aggregates to liberate them into the water column and 2) size-selective transport. Only the second process is considered in this model. Not exactly, the sediment transport process is lumped. We argue that this is appropriate for the scales (primarily temporal) we simulate. Soilscape evolution is extremely complex and numerical models cannot, and are not intended to, exactly and fully mimic it. Models are useful for simplifying complex dynamics, allowing us to isolate parameters and processes and test hypotheses and concepts. Modeling results must be interpreted within the model assumptions, a concept that we carefully follow.

The model does not include the vertical redistribution of aeolian material (aeolian deposits stay on the surface). In nature, the reason why an argillic horizon forms is that aeolian fines are redistributed downward in the soil profile. Therefore, I don't see how this is a realistic model for pedogenesis. Same comment as above, consider the scales and focus of this study.

Calibration concerns:

Some of the model parameters are chosen ad hoc (i.e. beta = 0.1, n_4 = 0.1) with no apparent calibration. Some are simply chosen based on the default values in other studies that may or may not be realistic for the study site in Israel. No data were used to relate climate changes to the model parameters. The "change factor" values and how they were modified over time may be qualitatively correct but the absolute values appear to be ad hoc. Some data must be used for calibration. Expending on our previous comments, the goal of this study is not to precisely predict soil dynamics but rather to isolate and conceptually analyze specific processes and dynamics. That can only be done with numerical models given the complexity and longevity of many of the processes involved. Over the years we have used best available data to calibrate some of the model parameters. In a limited and qualitative ways this is what we have done here with observed soil distribution. However we have found that using observed data to calibrate a specific model parameter is extremely problematic as, almost always, the parameter dynamics (spatial and temporal) cannot be sufficiently isolated form the observations. For this field site we actually have quite detailed paleoclimate and hydrological data (references are provided in the manuscript) but we intestinally simplified it. We did so for two reasons: (1) it allows for a much clearer analysis and (2) we are not attempting to precisely predict soilscape dynamics. This again relate to our previous comment about the use of models for soilscape evolution studies.

More broadly, the model has so many parameters (I lost count – a table of parameters, their units, and their chosen values would have helped) that I cannot see how a search of the parameter space could possibly have been done to find the optimal values, except via a Bayesian approach such as MCMC. Calibrating a model with 10 or 20+ parameters to a dataset that constrains only one element of the system (soil depth in this case) has to be done very carefully if it can be done at all. In cases where model parameters were matched to the observed data using an "extensive parametric study", no details are provided. This makes it very difficult to have confidence in the conclusions. When the model "fails" to match the data for the fluvial case or the diffusive case, perhaps it is simply that the model hasn't been properly calibrated. See comment above, these issues were address in the last four papers about this model.

The paper concludes that different parts of the hillslopes tend to be dominated by one of the two transport mechanisms; diffusion at the top and fluvial at the bottom. I don't see how the numerical experiments support the conclusion that fluvial processes dominate at the bottom. This is explained at the results and discussion sections: each of the transport mechanisms resulted (when simulated alone) in fairly distinct soil dynamics. When the two were simulated together their signatures were visible in different parts of the soilscape.

This conclusion is inconsistent with Tarboton et al. (1992) and many more recent studies (Perron et al., 2008; 2009) that conclude that the transition from diffusive to fluvial dominance occurs at the channel head. As long as one is on an unincised hillslope, diffusive processes should be dominant everywhere according to the published literature.

Good, now you are getting to a main goal of this paper – investigating the potential differences between aeolian and bedrock ("normal") soilscape evolution. These comments support our assertion and results that the two are indeed different - though the references and your comment focus on channel-hillslope interaction and we are only looking at hillslope processes here. We admit that the use of the term 'fluvial' is confusing in this context but we explicitly explain this in the introduction. This is stated and discussed in the manuscript, even in the context of our previous study: "In Cohen et al., (2015) we found an opposite trend for bedrock weathering dominated soilscapes." (section 4. Discussion).

The discrepancy between the results of this paper and previous studies could simply be a result of the very unrealistic value of beta (0.1) chosen with no justification. As stated above we did provide justification to beta. See comment above about equation 4.

Certainly fluvial erosion must become relatively more important at the base of the slopes compared to the top because the contributing area goes to zero at the top (hence the importance of fluvial transport must go to zero at the divide). True but this is a highly spatially and temporally dynamic change, not as simple as you describe it.

However, I do not see any evidence in the paper that fluvial processes dominate diffusive processes at the base of the slope. This is discussed in the manuscript. In a nutshell: if you compare soil depth evolution between the three simulations (Figures 4-6) and the cross section results (Figure 7) you will see that diffusion led to thick soils at the base in contrast to the fluvial simulation. The combined simulation looks a lot like the fluvial simulation at the base and like the diffusive at the middle part of the hillslope. We acknowledge that this is a qualitative observation but (as commented above about model assumptions and simplifications) we assert that it is most appropriate.

Other concerns:

The authors state that soil development is dominated by aeolian processes at their study site but no evidence is provided to demonstrate this. There are now a number of studies that use immobile elements (Ti, Zr) to quantify the relative dominance of aeolian input versus in situ weathering of parent material in soils. So, it may be possible to constrain this yet I don't see how this was done in this study. The loess belt in the northern Negev has been well studied; including the rates, extent and dynamics of aeolian deposition in this region (some references are provided in the manuscript). Indeed all one need to do is walk the site and see the extent of loess deposition and how little soil is produced by bedrock weathering. That been said (and repeating an earlier responses), this is actually not a crucial point for this conceptual study.

Similarly, the key motivating question of the study is whether soil degradation is caused by climate change or anthropogenic forcing. I don't see any evidence in this paper that soils were depleted (i.e. that they were thicker and have now thinned). Moreover, the question of whether soil degradation occurred by climate change or human activity relates primarily to the timing of the soil degradation. There is no geochronology or other evidence presented to address this question. These are two examples of many in

which facts were assumed about the study site without evidence. No, this is the overarching motivation not the goal of this study. The goal of this study is to gain conceptual insights into the soilscape evolution and the impacts of time varying parameters. As described above, we intentionally used broad-brush estimates of climatic and anthropogenic changes. Ongoing research (which will couple field and modeling efforts) is looking into the question of whether or not soil ever accumulated on the hillslopes. These points are clearly stated in the manuscript.

I don't understand why the observed soil depth (Fig. 7D) shows "spikes" in the plot. The color map from Fig. 2 does not show these spikes in the data. The soil map (Fig 2) is the product of interpolation between measurement points with exposed bedrock (classified form aerial photography) "burned" as zero depth (white color in Fig 2). This was explained in section 2.1. If you look closely you could see these zero-slope ("spikes") along the transect.

Anonymous Referee #2

This paper presents a simulation of soil-landscape evolution in a semiarid zone of Israel under fluvial and diffusive sediment transport.

The paper is nicely written and the method is clearly described. The results are stimulating, offering possible soil-landscape evolution pathways.

First of all we would like to thank the referee for this thorough review. Below we provide a point-by-point response to the reviewer's comments.

My comments are that some of the parameters are arbitrarily chosen, e.g. the humped model of weathering. While theoretically it is sound, but no published result yet showing such weathering parameters. As discussed at length in the response for review #1, it is true (and acknowledged in the manuscript) that many of the model parameters cannot be explicitly and directly calibrated even if extensive field data was available. This stems from the difficulty in isolating specific parameters from field observations, the longevity of the processes simulated and their complex interconnectivity and spatiotemporal dynamics. That is one of the motivations for developing a soilscape evolution model and for this study, isolating processes and parameters, allowing us to develop (and conceptually test) hypotheses on soilscape evolution pathways and drivers. That being said we have, over the last several years, focused our analysis on specific processes and parameters, gaining important insights into some of the model parameters. Most specifically, and relating to this comment, is our extensive analysis of weathering equations and parameters in Cohen et al. (2010). Moreover the hump weathering equation we used was adopted from Minasny and McBratney (2006) which is based on their extensive research.

The authors wrote: "Limestone bedrock typically results in limited soil production by weathering except for producing a Mollisol" The statement on limited production and Mollisol is not necessary true, Mollisol development is due to accumulation of loess and

organic matter. So why is this not true? We state: "…typically results in…" and go on to explain what is and is not actually simulated.

Another limited assumption is aeolian deposition which is uniform, what are the particle sizes of the aeolian deposit? Silt-size? 2-20 um? Good point. The aeolian deposition PSD is the same as the one we used in Cohen et al. (2015) and is shortly described there. We now clarify that in the manuscript: "We use the same PSD as in the fine-grained simulation in Cohen et al., (2015), with a d_{50}=0.06 mm." (section 2.1.3).

The simulation is run for 16,000 years. It would be beneficial to see how much of the "soil" is due to bedrock weathering and how much is due to aeolian deposit. As describe in section 2.4, bedrock weathering is assumed to be very low (0.01 mm/y), an order of magnitude lower tan aeolian deposition (0.1 mm/y). Also an explicit analysis of the two soil production mechanisms was explored in Cohen et al. (2015).

There is no mention of vegetation effect? Is there a possible feedback between vegetation and erosion? Of course, as well with bioturbation, crusts etc. These kind of caveats were discussed quite extensively in previous papers (particularly in Cohen et al., 2015). This fact is now described in the manuscript.

Main document changes and comments

Page 4: Deleted **Sagy Cohen** **3/29/16 10:32 AM**

(%)

Page 4: Inserted **Sagy Cohen** **3/29/16 10:32 AM**

(m/m)

Page 4: Deleted **Sagy Cohen** **3/28/16 11:31 AM**

modeling

Page 4: Inserted **Sagy Cohen** **3/28/16 11:31 AM**

modelling

Page 4: Inserted **Sagy Cohen** **3/28/16 11:32 AM**

The mARM framework introduced a novel implementation of physically-based equations using transition matrices that express the relative change in spatially and temporally explicit PSD vectors. This concept greatly improves the model computational efficiency and modularity but is challenging to describe in full. Below we describe the mARM5D physically-based equations that include the parameters that are modified in the simulation scenarios we analysed in this paper.

Page 4: Deleted **Sagy Cohen** **3/28/16 11:40 AM**

.

Page 4: Inserted **Sagy Cohen** **3/28/16 11:40 AM**

:

Page 5: Inserted **Sagy Cohen** **3/22/16 4:58 PM**

In Cohen et al. (2015) also outline and discuss the model assumptions.

Page 5: Deleted **Sagy Cohen** **3/28/16 11:37 AM**

Below we describe the mARM5D equations that include the parameters that are modified by the simulation scenarios we analysed here.

Page 5: Deleted **Sagy Cohen** **3/24/16 11:51 AM**

by

Page 5: Inserted **Sagy Cohen** **3/24/16 11:51 AM**

using a modification of the TOPOG model (TOPOG, 1997) sediment transport equation

Page 5: Deleted **Sagy Cohen** **3/24/16 11:52 AM**

a modified *Engelhund and Hansen* (1968) equation:

Page 5: Inserted **Sagy Cohen** **3/22/16 5:30 PM**

$$q_s = e\frac{q^{n_1}S^{n_2}}{(s-1)^2{d_{50}}^{n_3}}$$

Page 5: Inserted **Sagy Cohen** **3/29/16 9:33 AM**

(m/m)

Page 5: Inserted	Sagy Cohen	3/28/16 2:44 PM

$$\left[\frac{A}{A_p}\right]^{n_4} \frac{Q}{(A_p)^{0.5}}$$

Page 6: Deleted	Sagy Cohen	3/28/16 11:43 AM

modeled

Page 6: Inserted	Sagy Cohen	3/28/16 11:43 AM

modelled

Page 6: Formatted	Sagy Cohen	3/28/16 11:43 AM

Not Highlight

Page 6: Inserted	Sagy Cohen	3/24/16 2:30 PM

Page 6: Deleted	Sagy Cohen	3/28/16 11:13 AM

$$D_s = S^{\beta} k \Delta t$$

Page 6: Formatted	David

Lowered by 6 pt

Page 6: Inserted	Sagy Cohen	3/28/16 11:12 AM

$$D_s = \left(\frac{S}{S_a}\right)^{\beta} D_o \Delta t$$

Page 6: Inserted	Sagy Cohen	3/28/16 11:13 AM

Page 6: Inserted	Sagy Cohen	3/29/16 9:37 AM

Page 6: Deleted	Sagy Cohen	3/29/16 10:29 AM

Page 6: Inserted	Sagy Cohen	3/28/16 11:13 AM

D_o

Page 6: Deleted	Sagy Cohen	3/28/16 11:13 AM

k

Page 6: Inserted	Sagy Cohen	3/28/16 10:57 AM

(m) and S_a is the adjustment slope, the average slope in which D_o was measured/estimated

Page 6: Formatted	Sagy Cohen	3/29/16 10:33 AM

Font:Italic, Not Highlight

Page 6: Formatted	Sagy Cohen	3/29/16 10:33 AM

Not Highlight

Page 6: Inserted	Sagy Cohen	3/29/16 10:30 AM

Here we use S_a=0.2 which approximate our field site average slope.

Page 6: Formatted	Sagy Cohen	3/29/16 10:33 AM

Not Highlight

Page 6: Inserted	Sagy Cohen	3/29/16 9:28 AM

This value differs from the typical assumption of a linear relationship between slope and diffusion (β=1), suggesting that the influence of topographic slope in this soilscape is much lower. We will discuss this later.

Page 6: Formatted	Sagy Cohen	3/29/16 10:33 AM

Not Highlight

Page 6: Deleted	Sagy Cohen	3/28/16 2:45 PM

2.1.3 Weathering

The profile layers are subject to bedrock and soil weathering. We considered physical weathering calculated by breaking a parent particle into two daughter particles. As mass conservation is assumed, the diameters of the daughter particles (d_1, d_2) can be determined from the diameter of the parent particle (d_0). Based on experimental studies by *Wells et al.* (2008) we used a split-in-half geometry which leads to $d_1 = d_2$. A bedrock and soil weathering depth-dependency equation is used to set the weathering rate in each profile layer as a function of its depth below to the surface (*Heimsath et al.,* 1997). Following *Cohen et al*., (2010), we used a modified version of the 'humped' soil-production function (*Ahert*, 1977) proposed by *Minasny and McBratney* (2006):

$$W_l = P_0\left[\exp(-\delta_1 h_1 + P_a) - \exp(-\delta_1 h_1)\right] \quad (5)$$

where W_l is the physical weathering rate for profile layer l, P_0 and P_a (mm/yr) is the potential (or maximum) and steady-state weathering rates respectively, h_l (m) is the depth below the surface for layer l and δ_1 and δ_2 are constants. The values proposed by *Minasny and McBratney* (2006), δ_1=4, δ_2=6, are used here.

Page 6: Formatted	Sagy Cohen	3/23/16 11:41 AM

Highlight

Page 6: Formatted	Sagy Cohen	3/23/16 11:41 AM

Highlight

Page 6: Inserted	Sagy Cohen	3/28/16 2:45 PM

Page 6: Inserted	Sagy Cohen	3/28/16 2:44 PM

$h_s \underline{g_s}_{t+1}$

Page 6: Inserted	Sagy Cohen	3/28/16 2:44 PM

$h_s \underline{g_s}_{t}$

Page 6: Inserted	Sagy Cohen	3/28/16 2:44 PM

$K_a \underline{g}_{a}$

Page 6: Inserted	Sagy Cohen	3/28/16 2:44 PM

$\underline{g_s}_{t}$

Page 6: Inserted	Sagy Cohen	3/22/16 11:05 AM

We use the same PSD as in the fine-grained simulation in Cohen et al., (2015), with a d_{50}=0.06 mm (derived from Bruins and Yaalon, 1992)

.

Page 6: Formatted	Sagy Cohen	3/29/16 10:25 AM

Subscript

Page 7: Inserted	Sagy Cohen	3/28/16 11:17 AM

0

Page 7: Deleted	Sagy Cohen	3/28/16 11:17 AM

s

Page 7: Inserted	Sagy Cohen	3/28/16 11:18 AM

0

Page 7: Deleted	Sagy Cohen	3/28/16 11:18 AM

s

Page 7: Inserted	Sagy Cohen	3/28/16 11:18 AM

D_0

Page 7: Deleted	Sagy Cohen	3/28/16 11:18 AM

D_s

Page 7: Inserted	Sagy Cohen	3/28/16 11:18 AM

D_0

Page 7: Deleted	Sagy Cohen	3/28/16 11:18 AM

D_s

Page 7: Inserted	Sagy Cohen	3/28/16 11:18 AM

D_0

Page 7: Deleted	Sagy Cohen	3/28/16 11:18 AM

$\boldsymbol{D_s}$

Page 7: Inserted	Sagy Cohen	3/28/16 11:18 AM

$\boldsymbol{D_0}$

Page 7: Deleted	Sagy Cohen	3/28/16 11:18 AM

$\boldsymbol{D_s}$

Page 8: Inserted	Sagy Cohen	3/28/16 11:18 AM

D_0

Page 8: Formatted	Sagy Cohen	3/28/16 11:19 AM

Font:Not Bold

Page 8: Deleted	Sagy Cohen	3/28/16 11:18 AM

D_s

Page 8: Inserted	Sagy Cohen	3/28/16 11:20 AM

D_0

Page 8: Deleted	Sagy Cohen	3/28/16 11:20 AM

D_s

Page 8: Inserted	Sagy Cohen	3/28/16 11:18 AM

D_0

Page 8: Formatted	Sagy Cohen	3/28/16 11:18 AM

Font:Not Bold

Page 8: Deleted	Sagy Cohen	3/28/16 11:18 AM

D_s

Page 8: Inserted	Sagy Cohen	3/28/16 11:19 AM

D_0

Page 8: Deleted	Sagy Cohen	3/28/16 11:19 AM

D_s

Page 8: Inserted	Sagy Cohen	3/28/16 11:19 AM

D_0

Page 8: Deleted	Sagy Cohen	3/28/16 11:19 AM

D_s

Page 11: Inserted	Sagy Cohen	3/29/16 10:09 AM

Page 11: Deleted	Sagy Cohen	3/29/16 10:21 AM

Page 11: Deleted	Sagy Cohen	3/29/16 10:06 AM

armored

Page 11: Inserted	Sagy Cohen	3/29/16 10:06 AM

armoured

Page 11: Inserted	Sagy Cohen	3/29/16 10:22 AM

Diffusion rate for this field site was found (based on an extensive parametric study) to have a weak and nonlinear relationship with topographic slope (β=0.1 in Eq. 4). This differs from the usual assumption of linearity (e.g. ref.) and may be due to the aeolian characteristics of the site's soilscape (fine PSD, absence of armouring mechanism, etc.) or may be attributed to the relatively steep and concave-down (increase in gradient downslope) characteristics of this field site. This will be the focus of a future study.

Page 11: Formatted	Sagy Cohen	3/29/16 10:24 AM

Highlight

Page 13: Formatted	Sagy Cohen	3/22/16 4:56 PM

Font:10 pt

Page 13: Formatted	Sagy Cohen	3/22/16 4:56 PM

Font:10 pt

Page 14: Formatted	Sagy Cohen	3/22/16 4:56 PM

Font:10 pt

Page 14: Deleted	Sagy Cohen	3/22/16 10:23 AM

Engelhund, F., and E. Hansen (1968), A Monograph on Sediment Transport in Alluvial Streams. Teknish Forlag, Technical Press, Copenhagen, Denmark 62 pp.

Page 14: Formatted	Sagy Cohen	3/22/16 4:56 PM

Font:10 pt

Page 15: Formatted	Sagy Cohen	3/22/16 4:56 PM

Font:10 pt

Page 15: Inserted	Sagy Cohen	3/22/16 5:54 PM

Minasny, B., and McBratney, A.B. (2006), Mechanistic soil-landscape modelling as an approach to developing pedogenesis classifications. *Geoderma*, 133: 138-149.

Page 15: Formatted	Sagy Cohen	3/22/16 5:54 PM

Normal, Indent: Left: 0", Hanging: 0.31"

Page 15: Formatted	Sagy Cohen	3/22/16 4:56 PM

Font:10 pt

Page 15: Formatted	Sagy Cohen	3/22/16 4:56 PM

Font:10 pt

Page 15: Formatted	Sagy Cohen	3/22/16 4:56 PM

Default Paragraph Font

Page 15: Inserted	Sagy Cohen	3/24/16 11:55 AM

TOPOG (1997): http://www-data.wron.csiro.au/topog/user/user.html

Page 15: Formatted	Sagy Cohen	3/22/16 4:56 PM

Font:10 pt

Header and footer changes

Text box changes

Header and footer text box changes

Footnote changes

Endnote changes

Soilscape evolution of aeolian-dominated hillslopes during the Holocene: investigation of sediment transport mechanisms and climatic-anthropogenic drivers

Sagy Cohen[1,2*], Tal Svoray[2], Shai Sela[2], Greg Hancock[3] and Garry Willgoose[4]

[1] Department of Geography, University of Alabama, Box 870322, Tuscaloosa, Alabama 35487, USA.

[2] Department of Geography and Environmental Development, Ben-Gurion University of the Negev, Israel.

[3] School of Engineering, The University of Newcastle, Callaghan, New South Wales 2308, Australia

[4] School of Environmental and Life Sciences, The University of Newcastle, Callaghan, New South Wales 2308, Australia

* Corresponding author:

Email: sagy.cohen@ua.edu; Phone: 1-205-348-5860; Fax: 1-205-348-2278

Keywords: Soilscape, Pedogenesis, Sediment Transport, Modeling, Aeolian, Loess.

Submitted to: Earth Surface Dynamics

Abstract

Here we study the soilscape (soil-landscape) evolution of a field-site at the semiarid zone of Israel. This region, like similar regions around the world, was subject to intensive loess accumulation during the Pleistocene and early Holocene. Today, hillslopes in this region are dominated by exposed bedrock with deep loess depositions in the valleys and floodplains. The drivers and mechanism that led to this soilscape are unclear. Within this context, we use a soilscape evolution model (mARM5D) to study the potential mechanisms that led to this soilscape. We focus on advancing our conceptual understanding of the processes at the core of this soilscape evolution by studying the effects of fluvial and diffusive sediment transport mechanisms, and the potential effects of climatic and anthropogenic drivers. Our results show that in our field site, dominated by aeolian soil development, hillslope fluvial sediment transport e.g. surface wash and gullies, lead to downslope thinning in soil while diffusive transport e.g. soil creep lead to deeper and more localized soil features at the lower sections of the hillslopes. The results suggest that, in this semiarid, aeolian-dominated and soil depleted landscape, the top section of the hillslopes is dominated by diffusive transport and the bottom by fluvial transport. Temporal variability in environmental drivers had a considerable effect on soilscape evolution. Short but intensive changes during the late Holocene, imitating anthropogenic landuse alterations, rapidly changed the site's soil distribution. This leads us to assume that this region's soil depleted hillslopes are, at least in part, the result of anthropogenic drivers.

1. Introduction

Southern Israel, similar to other regions around the world, was subject to intensive loess accumulation during the Pleistocene and early Holocene. Hillslopes in this region are currently dominated by exposed bedrock with deep loess deposits in the valleys. The drivers and timing of the soilscape evolution that led to this soilscape are debatable. Studies in southern Europe and in the northern parts of the Middle East have found that anthropogenic activities (e.g. shrub removal, logging/timber extraction and over grazing in the late Holocene) were the dominant driver for the extensive removal of soils from hillslopes in many regions (*Fuchs et al*., 2004; *Fuchs*, 2007; *van Andel et al*., 1990). These conclusions differ from studies in the Negev Desert in Israel which found that most of the hillslope loess apron was eroded in the early Holocene, prior to significant human settlement (*Avni et al*. 2006). This finding suggests that the degradation of soil from the Negev Desert hillslopes, where such existed, was driven by climatic, rather than anthropogenic processes. Consequently, there is an ongoing debate in the literature regarding the drivers of the extensive soil depletion in Mediterranean and southern European hillslopes.

From a soilscape evolution point of view, aeolian dominated soilscapes differ from bedrock-weathering dominated soilscapes in several ways. In bedrock-weathering systems *in situ* weathering rates decrease exponentially with soil depth (*Gilbert*, 1877; *Ahnert*, 1977), thus regulating soil production as a function of regolith thickness (*Heimsath et al*., 1997). Weathering of regolith and soil leads to vertical particle size distribution with finer particles closer to the surface as a

function of the soil and regolith age, namely time exposed to weathering (*Yoo and Mudd* 2008). At the surface, armouring can develop by size-selective entrainment (*Kim and Ivanov*, 2014) or vegetation shielding, which limits sediment transport by overland flow (*Willgoose and Sharmeen*, 2006). Given sufficient time and in the absence of vertical mixing due to pedoturbation, these processes - depth dependent weathering, vertical self-organization and surface armouring - will stabilize the soilscape leading to steady-state or dynamic equilibrium conditions (*Cohen et al*., 2013 & 2015). In aeolian dominated landscapes these controls on soil production and transport are largely ineffective as: (1) much of the soil is transported to the system as airborne sediments, i.e., no depth dependency; and (2) fine and highly erodible material is continuously deposited on top of older surface soils which limits the potential for surface armouring and vertical self-organization.

The differences between aeolian and bedrock-weathering dominated soilscapes lead us to conclude that traditional (i.e. bedrock weathering originated) soilscape evolution analysis is inappropriate for investigating the history of the aforementioned loess soilscapes. In *Cohen et al.* (2015) we developed a soilscape evolution model (mARM5D) to study the differences and interactions between aeolian and bedrock weathering soil production on a synthetic 1D hillslope. In that paper we have found that bedrock weathering dominated soilscapes are considerably more stable and showed much lower spatial (aerial) variability in soil depth and particle size distribution (PSD). We proposed that aeolian-dominated landscapes are more responsive to environmental changes (e.g., climatic and anthropogenic) compared with bedrock-weathering landscapes.

Here we use mARM5D to investigate an aeolian dominated field-site in central Israel located at the margin between Mediterranean and arid climates and with long history of human settlement. We introduce anthropogenic and climatic drivers to investigate the potential importance of temporal dynamics on soilscape evolution. We focus our analysis in this paper on the differences between Fluvial (rilling, hillslope wash and concentrated flow) and Diffusive (soil creep) hillslope sediment transport mechanisms. We seek to gain better understanding about how these sediment transport mechanisms affect soilscape evolution in this soilscape. This is important as: (1) each transport mechanism is affected differently by climatic/anthropogenic drivers; and (2) we do not know what is the potential contribution/importance of each mechanism on soilscape evolution.

2. Methodology

2.1 Field site and measured data

The field-site (Long Term Ecological Research, LTER, near Lehavim in the Northern Negev, Israel; $31^{0}20'$ N, $34^{0}45'$ E; Figure 1) is situated on the desert margin between a Mediterranean climatic regime to the north and an arid climatic regime to the south (note changes in green vegetation in Figure 1a). The area of the site is 0.115 km^2. This region has shifted between these two climatic regimes throughout the Pleistocene and Holocene (*Vaks et al*., 2006). This region has also seen varying degrees of human settlement and agricultural activity throughout the late Holocene. The history of this region (both

human and natural) gives us a unique opportunity to study how climatic and anthropogenic drivers may have affected hillslope geomorphology resulting in the soil-depleted landscape we see today.

The LTER site is located in Aleket basin with an average rainfall of 290 mm per annum. The mean annual temperature is 20.5^{0}C, with a maximum of 27.5^{0}C and a minimum of 12.5^{0}C. The terrain is hilly and the area is divided by an east-west flowing ephemeral stream. The dominant rock formations are Eocenean limestone and chalk with patches of calcrete. Soils are brown lithosols and arid brown loess. Much of the loess was eroded from the hillslopes and deposited in the valleys (several meters deep in some locations). The vegetation is characterized by scattered dwarf shrubs (dominant species *Sarcopoterium spinosum*) and patches of herbaceous vegetation, mostly annuals, are spread between rocks and dwarf shrubs (*Svoray et al*. 2008). The herbaceous vegetation is highly diverse, mostly composed of annual species (*Svoray and Karnieli 2011*). At the research site a typical convex shaped slope was chosen for testing model predictions (Figure 1d).

A dataset of measured topography and soil parameters at the study site (including soil depth distribution and a Digital Elevation Model; DEM) is available from a previous study (*Sela et al*. 2012). A soil depth map (Figure 2) was compiled using Ordinary Kriging interpolation of 550-point measurements. An orthophoto (at 10 cm^2 pixel resolution) was use to classify exposed rock and assign zero depth to the interpolation map. The DEM used in this study was obtained from 700 measured points (at approximately 10 meter intervals) using a laser theodolite (SOKIA Inc. Total Station) and interpolated using Ordinary Kriging to a horizontal resolution to 2 x 2 meter pixel resolution for the mARM5D simulations. From this DEM a D8 flow direction, Dinf (D-infinity algorithm; *Tarboton,* 1997) slope (m/m) and Dinf contributing area layers were calculated using the TauDEM tool (Tarboton, 2010).

Sagy Cohen 3/29/2016 10:32 AM
Deleted: (%)

2.2 Application of mARM5D to Lehavim site

In *Cohen et al*. (2015) we developed a dynamic soil evolution model (mARM5D) to simulate soil physics as a state-space system as an extension of the mARM3D model (*Cohen et al*., 2009; 2010). mARM5D is a modular and computationally efficient modelling platform that explicitly simulates three spatial dimensions in addition to a temporal dimension and a PSD (hence the 5D suffix). The cellular model simulates soil evolution over a given landscape by describing changes in PSD in a finite number of equally thick soil profile layers (size and number are defined by the user) in each grid-cell.

Sagy Cohen 3/28/2016 11:31 AM
Deleted: modeling

The mARM framework introduced a novel implementation of physically-based equations using transition matrices that express the relative change in spatially and temporally explicit PSD vectors. This concept greatly improves the model computational efficiency and modularity but is challenging to describe in full. Below we describe the mARM5D physically-based equations that include the parameters that are modified in the simulation scenarios we analysed in this paper. A full description of the mARM model architecture as a platform to mARM5D can be found in the following publications: The model weathering component was explored in Cohen et al. (2010), its spatiotemporal algorithms in Cohen et al. (2013) and

Sagy Cohen 3/28/2016 11:40 AM
Deleted: .

its aeolian and sediment transport components in Cohen et al. (2015). In Cohen et al. (2015) also outline and discuss the model assumptions.

Here, we simulate the spatial and temporal changes in PSD as resulting from: (1) physical weathering of bedrock and soil particles in each profile-layer; (2) aeolian deposition on top of the surface layer; (3) size-selective entrainment and deposition by overland flow (generally referred to here as fluvial sediment transport) from/on the surface layer; and (4) non size-selective diffusive sediment transport (creep) both on the surface and within the soil profile.

Sagy Cohen 3/28/2016 11:37 AM
Deleted: Below we describe the mARM5D equations that include the parameters that are modified by the simulation scenarios we analysed here.

2.1.1 Fluvial transport

For each grid-cell, the top layer is the surface layer exposed directly to size-selective erosion. Sediment transport capacity over a timestep (q_s, m^3/m) at the surface is calculated using a modification of the TOPOG model (TOPOG, 1997) sediment transport equation

Sagy Cohen 3/24/2016 11:51 AM
Deleted: by

Sagy Cohen 3/24/2016 11:52 AM
Deleted: a modified *Engelhund and Hansen* (1968) equation:

$$q_s = e\frac{q^{n_1}S^{n_2}}{(1-s)^2 d_{50}^{\ n_3}}\Delta t \qquad q_s = e\frac{q^{n_1}S^{n_2}}{(s-1)^2 d_{50}^{\ n_3}} \qquad (1)$$

where e is an empirical erodibility factor, q is discharge per unit width ($m^3/s/m$), S is slope (m/m), d_{50} is the median diameter (m) of the material in the surface layer, s is the specific gravity of sediment (s=2.65; kg/m^3), n_1, n_2 and n_3 are calibration parameters and Δt is the timestep size. The units of erodibility parameter e are a function of the calibration exponents n^1, n^2 and n^3 and are defined such that the units of q_s are the ones specified. We used here n_1=1 and n_2=1.2 based on a calibration in *Cohen et al*. (2009) and modified n_3 to 0.5 (from 0.025) to adjust for the very fine-grained aeolian sediment.

Discharge (q; $m^3/s/m$) is

$$q = \left[\frac{A}{A_p}\right]^{n_4}\frac{Q}{(A_p)^{0.5}} \qquad (2)$$

where Q (m^3/s) is the excess hillslope runoff variable, A is the upslope contributing area (m^2), A_p is the area of a grid cell unit (m^2) and n_4 is a constant relating runoff as a function of contributing area. In *Cohen et al*. (2010 and 2015) the relationship between contributing area and runoff discharge was assumed to be linear (n_4=1). This assumption could not be justified in our field-site as *Yair and Kossovsky* (2002) showed that runoff generation in this region does not increase linearly downslope. We therefore use n_4=0.1 in this study. Water is routed to a neighboring grid-cell with the 'steepest descent' (D8) algorithm (*O'Callaghan and Mark*, 1984)

2.1.2 Diffusion transport

Traditionally, equations of two-dimensional diffusive transport calculate sediment discharge as a linear relationship to slope, soil thickness and a diffusion coefficient (e.g. the creep model of *Culling*, 1963, or the viscous flow model of *Ahnert*, 1976) and, if the soil is explicitly modelled at all, diffusion is considered independent of depth through the profile. Simulation of the soil profile in mARM5D is novel as it explicitly calculates diffusive transport for each soil profile layer. Based on *Roering* (2004), the diffusivity is assumed to decrease exponentially with depth below the soil surface:

$$D_l = D_s[\exp(-\lambda h_l)] \quad (3)$$

where D_l (m/y) is the diffusive transport rate for the layer l, D_s is the surface (maximum) diffusive sediment transport rate (m/y), h_l is the mean depth (m) of profile layer l relative to the surface and λ is a calibration parameter. We used λ=0.02 based on *Fleming and Johnson* (1975) and *Roering* (2004). The surface diffusion sediment transport rate (D_s; m/y) is:

$$D_s = \left(\frac{S}{S_a}\right)^{\beta} D_o \Delta t \quad (4)$$

where D_o is the surface diffusivity (m) and S_a is the adjustment slope, the average slope in which D_o was measured/estimated. Here we use S_a=0.2 which approximate our field site average slope. Using an extensive sensitivity analysis we have found that β=0.1 yielded the best approximation to our field site's soil distribution. This value differs from the typical assumption of a linear relationship between slope and diffusion (β=1), suggesting that the influence of topographic slope in this soilscape is much lower. We will discuss this later. Sediment flux for each layer can be calculated by multiplying D_s by the volume and the bulk density of the soil. We assumed constant volume and bulk density.

2.1.3 Aeolian deposition

Sediment, with a user-defined grading distribution ($\underline{g}_a$), is added to the surface layer. The aeolian deposition rate (K_a; mm/yr) is assumed to be spatially uniform:

$$h_s \underline{g_s}_{t+1} = h_s \underline{g_s}_t + K_a \underline{g}_a \quad (6)$$

where $\underline{g_s}_t$ is the vector for the surface layer PSD and h_s is the thickness of the surface layer. We use the same PSD as in the fine-grained simulation in Cohen et al., (2015), with a d_{50}=0.06 mm (derived from Bruins and Yaalon, 1992) . For the sake of simplicity, aeolian sediment is assumed to originate from outside the system and no aeolian erosion is considered within the simulated domain. This means that K_a is, in our case, the aeolian sediment accumulation (deposition) rate.

Sagy Cohen 3/28/2016 11:43 AM
Deleted: modeled

Sagy Cohen 3/28/2016 11:43 AM
Formatted: Not Highlight

Sagy Cohen 3/28/2016 11:13 AM
Deleted: $D_s = S^{\beta} k \Delta t$

Unknown
Formatted: Lowered by 6 pt

Sagy Cohen 3/29/2016 10:29 AM
Deleted:

Sagy Cohen 3/28/2016 11:13 AM
Deleted: *k*

Sagy Cohen 3/29/2016 10:33 AM
Formatted: Font:Italic, Not Highlight

Sagy Cohen 3/29/2016 10:33 AM
Formatted: Not Highlight

Sagy Cohen 3/29/2016 10:33 AM
Formatted: Not Highlight

Sagy Cohen 3/29/2016 10:33 AM
Formatted: Not Highlight

Sagy Cohen 3/28/2016 2:45 PM
Deleted: 2.1.3 Weathering ... [1]

Sagy Cohen 3/23/2016 11:41 AM
Formatted: Highlight

Sagy Cohen 3/23/2016 11:41 AM
Formatted: Highlight

Sagy Cohen 3/29/2016 10:25 AM
Formatted: Subscript

2.3 Simulation scenarios

Four model parameters are driven by climate and anthropogenic changes:

1. $\boldsymbol{e}$ - Surface Erodibility (equation 1);
2. $\boldsymbol{Q}$ – Runoff (equation 2);
3. $\boldsymbol{D_{0y}}$ – Surface diffusive transport rate (equation 3 and 4);
4. $\boldsymbol{K_a}$ – Aeolian deposition rate (equation 5).

The effect of climate and anthropogenic change on the model parameters represent our best estimates based on the literature for this semiarid region. They can be summarized as:

1. Wetter climatic conditions allow for higher vegetation cover and thus lower surface erodibility and runoff generation ($\boldsymbol{e}$ and $\boldsymbol{Q}$ respectively) (*Goodfriend*, 1987, *Zilberman*, 1992 and *Avni et al*., 2006).
2. During wetter climatic condition colluvial processes are more intensive (*Goodfriend*, 1987 and *Zilberman*, 1992), translating into a higher diffusive sediment transport rate ($\boldsymbol{D_{0y}}$).
3. During wetter climatic condition aeolian deposition rates are higher ($\boldsymbol{K_a}$) (*Horowitz*, 1979 and *Bowman et al*., 1986).
4. Human activities in this area reduce vegetation cover on the hillslopes (mostly by grazing), enhancing the effect of the dry climate during the Holocene (*Fuchs et al*., 2004), increasing $\boldsymbol{e}$ and $\boldsymbol{Q}$ and decreasing D_{0y} and $\boldsymbol{K_a}$.

Using these assumptions we divided the simulation scenario into three homogenous periods (Figure 3 and Table 1) based on *Vaks el al*. (2006):

P1- Late Pleistocene (80-12 kyr BP): wetter climatic period – a factor of 0.1 for erosivity and runoff ($\boldsymbol{e}$ and $\boldsymbol{Q}$ respectively), scale of 2 for diffusion (D_{0y}) relative to modern rates and a maximum rate for aeolian deposition ($\boldsymbol{K_a}$).

P2 - Early Holocene (12-8 kyr BP): dry climatic period - scale of 0.2 for $\boldsymbol{e}$ and $\boldsymbol{Q}$, factor of 2 for D_{0y} (unchanged from P1) relative to modern rates and scale of 0.5 for $\boldsymbol{K_a}$ relative to its P1 (maximum) rate.

P3 - Late Holocene (8-0 kyr BP): increasingly drier climate with human activity - scale of 1 (maximum) for $\boldsymbol{e}$ and $\boldsymbol{Q}$, scale of 1 for D_{0y} and factor of 0.1 for $\boldsymbol{K_a}$ relative to its P1 (maximum) rate.

2.4 Simulated processes and calibration

Three site-scale simulations are analyzed in this paper:

S1- sediment transport is simulated only by fluvial processes;

S2- sediment transport is simulated only by diffusion;

S3- sediment transport is simulated by both diffusive and fluvial mechanisms.

Soil is produced and supplied by both bedrock weathering and aeolian deposition. Soil production by bedrock weathering was assumed to be small relative to loess accumulation rate due to the dominance of limestone geology in the site.

Sagy Cohen 3/28/2016 11:17 AM
Deleted: $_s$

Sagy Cohen 3/28/2016 11:18 AM
Deleted: $_s$

Sagy Cohen 3/28/2016 11:18 AM
Deleted: D_s

Sagy Cohen 3/28/2016 11:18 AM
Deleted: D_s

Sagy Cohen 3/28/2016 11:18 AM
Deleted: D_s

Sagy Cohen 3/28/2016 11:18 AM
Deleted: D_s

Limestone bedrock typically results in limited soil production by weathering except for producing a Mollisol, which is not simulated, and rock fragments, which are simulated. Weathering rate (P_0 in equation 5) is thus set to spatially and temporally constant value of 0.01 mm/y. Maximum aeolian deposition rate (during P1 simulation scenario period) is spatially constant and set to 0.1 mm/y based on *Bruins and Yaalon* (1992).

Initial values during the P3 period (most modern) for Q was estimated based on *Eldridge et al*. (2002) and *Yair and Kossovski* (2002) and for D_s based on *Carson and Kirkby* (1972). Adjusting these two parameters controls the ratio between the fluvial and diffusive sediment transport mechanisms. The values of these parameters were refined by an extensive parametric study to best match observed soil depth distribution. The best match was for Q=0.0066 m^3/y and D_s=6 mm/y for the P3 period (Table 1).

For the S1 and S2 simulations, the Q and D_s parameters were adjusted to yield a similar average soil depth as the S3 simulation. This adjustment ensures that the differences observed between the three simulations are mainly due to differences in sediment transport mechanism, not the accumulative variations in sediment transport rate. For S1 Q was adjusted to 0.017 m^3/y and D_s was set to 0 (no diffusive transport; Table 1). For the S2 simulation D_s was adjusted to 10.75 mm/y and Q was set to 0 (no fluvial transport).

Sagy Cohen 3/28/2016 11:18 AM
Deleted: D_s

Sagy Cohen 3/28/2016 11:19 AM
Formatted: Font:Not Bold

Sagy Cohen 3/28/2016 11:20 AM
Deleted: D_s

Sagy Cohen 3/28/2016 11:18 AM
Formatted: Font:Not Bold

Sagy Cohen 3/28/2016 11:18 AM
Deleted: D_s

Sagy Cohen 3/28/2016 11:19 AM
Deleted: D_s

Sagy Cohen 3/28/2016 11:19 AM
Deleted: D_s

3. Results

3.1 Field Site Application

For the fluvial simulation (S1), the P1 period, with low runoff and surface erodibility and high aeolian deposition (Figure 3), produced deep soils on the hillslopes (up to 200 cm; Figure 4a-b). During P2, with higher runoff and surface erodibility rates and lower aeolian deposition rate (by a factor of 2), soil is slowly eroding primarily from the lower sections of the hillslopes (Figure 4c-d). Erosion greatly intensifies during P3 due to further increase in runoff and surface erodibility rates and lowering in aeolian deposition rate (by a factor of 5). By the end of P3, most of the thick hillslopes loess apron has been eroded (Figure 4f) leaving two clusters of relatively deep soils (about 150 cm deep) on the interfluve, as well as quite extensive shallow aprons (about 50 cm deep) at the top and middle sections of the hillslopes. The rest of the hillslope is covered with a shallow soil layer (<20 cm) with no exposed bedrock. This soil distribution does not correspond well with observed soil depth (Figure 2) which exhibits a high degree of exposed bedrock at the top section of the hillslopes and the interfluve and deeper soils at the lower parts of the hillslopes.

The diffusive simulation (S2) yielded long straight bands of soil deposition along parts of the domain. These bands follow the D8 flow direction input and are only apparent in the diffusive simulation. This seems to be because diffusive rate is highest during the P1 period in which aeolian deposition is also highest leading to the formation of deep deposition features down the flow lines. This observation is in contrast with the fluvial simulation in which highest fluvial transport

rates occur following a long period of extensive loess accumulation on the hillslopes (Figure 4b). This result emphasizes the importance of temporal dynamics in soil production and erosion.

The P1 period for the S2 simulation, with high diffusive and aeolian deposition rates, produced soil accumulation at lower sections of the hillslopes (Figure 5a-b). These deposition features are over 100 cm deep at the footslope and are decreasing in depth upslope. The upper sections of the hillslopes are covered with a shallow loess apron (< 20 cm) with narrow bands of exposed bedrock (white color) along the interfluve. During P2, aeolian deposition rate decreased while the diffusive rate remained high (Figure 3). This leads to erosion of the upslope deposition bands resulting in a slight decrease in their spatial extent (Figure 5c-d). The extent of the exposed bedrock feature along the crest and down the hillslopes increased. During P3, the diffusive rate decreases by a factor of 2 and aeolian deposition by a further factor of 5. The main impact of this reduced soil supply is an extensive degradation of the thin loess apron on the hillslopes (Figures 5e-f). The deposition bands at the bottom of the hillslopes are relatively unaffected. Final soil distribution (Figure 5f) better corresponds with the measured soil distribution (Figure 2) compared with the S1 simulation (Figure 4f). Measured soil depth tends to be more heterogeneous and widespread and does not show extremely localized deposition features at the footslopes.

In the combined fluvial and diffusive simulation (S3) the P1 period shows deep soil features, about 150 cm, covering most of the intermediate and lower sections of the hillslopes (Figure 6a-b). With an exception of a thin band of deep soils near the crest, the upslope parts are covered with a shallow loess apron (less than 15 cm). The changes during P2 (aeolian deposition decrease by a factor of 2, fluvial rate increase by a factor of 2 and diffusive rate remain high) initially led to degradation of the loess apron at the upper parts of the hillslopes (Figure 6c). Once the loess apron has been completely removed, the deposition features at the lower section of the hillslopes start to erode (Figure 6d). This trend accelerates during P3 due to the sharp decrease in aeolian deposition rate. The increase in fluvial rate by a factor of 5 while diffusive rate decreases by a factor of 2 (Figure 3) leads to greater erosion at the bottom parts of the deposition features (Figure 7e-f). The resulting soil distribution better corresponds with measured soil distribution: exposed bedrock at the top and bottom parts of the hillslopes with a mostly shallow band of soil at the middle part of the hillslopes. The considerable changes in soil depths during P3 shows that intense but relatively short changes in external drivers (representing anthropogenic alterations in this study) can be significant for this soilscape evolution.

3.2 Transect (1D) Analysis

Soil depth evolution was plotted along a transect on the northwestern facing hillslope (thick black line with crossing short lines in Figures 1c and 4-6), focusing on the last 16 kyr of the simulations (the most dynamic period of these simulations).

The S1 profile (Figure 7a) gradually thins toward the footslope while the S2 (Figure 7b) profile is very thin at the top of the hillslope and then thickens considerably from nearly zero depth to about 190 cm over a stretch of less than 5 m. The S3 simulation (Figure 7c) has also resulted in a steep step in soil depth between the upper and lower parts of the hillslope. However, the S3 simulation resulted in considerable variability in soil depth at the footslope. In the S1 simulation the

hillslope profile changes considerably during the plotted 16 kyr while the S2 profile displays only minor variation and S3 varies mainly at the bottom of the hillslope. The S1 hillslope profile initially erodes evenly in space but during P3 it shows increased erosion rate at the top of the hillslope. This trend is also visible in S3.

The final (0 kyr BP) hillslope profile for S3 has a nearly 35 m long exposed bedrock section at the top part of the hillslope (also visible in Figure 6f) followed by a deposition section with a downslope decreasing soil depth (from about 100 to 10 cm at the bottom of the hillslope). This profile has a number of both steep and shallow steps in soil depth (from more than a 100 cm to less than 10 cm) which are commonly observed in the Lehavim field-site. The measured soil depth profile along the transect (Figure 7d) is shallower and displays a smoother (it is an interpolation of measurement points) transition between the erosive and deposition parts of the hillslope. Overall the S3 soil-depth profile (Figure 8c) shows similar trends to the measured soil depth (Figure 7d). Particularly notable is the correspondence in the location of the mid-slope soil depth depression.

4. Discussion

Roering (2008) simulated soilscape evolution in a soil-mantled and vegetated landscape in northwestern U.S. He studied a number of diffusive sediment transport mechanisms and found that the best fit for the observed landform and soil distribution (increase in soil depth with slope angle downslope) was a nonlinear and soil depth-dependent model. He argued that soil thickness controls the magnitude of biogenetic activity (e.g. bioturbation) which drives sediment transport. In semiarid soil-depleted environments, landscape evolution and soil distribution was also found to be related to soil depth but by a different mechanism. *Saco et al.* (2007) simulated a semiarid and soil-depleted landscape and showed that soilscape evolution under water-limited conditions tend to follow a source-sink dynamics in which soil bands (which are deep enough to support vegetation) will act as a sink for water and sediment fluvially transported (surface wash) from bare intermediate sections between the vegetated bands.

The Lehavim LTER field site, under modern climatic conditions, is under a water-limited regime resulting in vegetation patches acting as sinks to the exposed bedrock section on the hillslope (*Svoray et al*., 2008; *Svoray and Karnieli,* 2011) leading to micro-topographic variability. The site's soilscape is also characterized by a general trend of increasing soil depths downslope. This suggests an intriguing interplay between semiarid and soil-mantled soilscape evolution. Our results show that during wetter periods (with greater aeolian deposition rates, P1) soil was thickening at the downslope direction (Figure 5b and Figure 6c). During the following drier periods (P2 and P3) the bottom part of the hillslopes started eroding resulting in a soil distribution where the middle part of the hillslope shows the deepest soil (the mid-slope depression; Figure 5 and 6). Simulated fluvial sediment transport led to a somewhat unusual soil distribution in which soil is thickest at the interfluve (Figure 4). Hints of this kind of soil distribution are evident in the Lehavim LTER site (e.g. north sections of both northwest and southeast facing hillslopes; Figure 2) but are not as prominent as the S1 simulation predicted. Diffusive transport tended

to produce localized deep deposition features at the bottom of the hillslopes. Evidence of this type of soil distribution can also be seen in this field-site (primarily on the southeast facing hillslope; Figure 2) though not as deep and localized as the S2 simulation (diffusive only sediment transport; Figure 5) produced. Only by simulating both fluvial and diffusive transport mechanisms can the model correctly simulate the observed soil distribution. Even though simulating both fluvial and diffusive sediment transport is common practice in many landscape-evolution models (*Tucker and Hancock*, 2010), the interaction between them is often uncertain (*Hancock et al.*, 2002), particularly under unique circumstances like in this field-site: fine-grained aeolian-dominated soils with high degree of temporal variation in soil supply.

The results show that different parts of the hillslopes tend to be dominated by one of the two transport mechanisms; diffusion at the top and fluvial at the bottom. In Cohen et al., (2015) we found an opposite trend for bedrock weathering dominated soilscapes. In bedrock weathering dominated soilscapes heterogeneity in PSD along the soil profile and selective entrainment by overland flow will result in less erosive (armoured) surface in response to increasing fluvial rates. Therefore increases in runoff rates downslope will not yield a considerable increase in sediment transport (rather an increasingly coarse, source-limited, surface). In aeolian dominated soilscapes the absence of such a mechanism means that increasing runoff downslope will, in the absence of other factors, result in increasing fluvial transport rates downslopes hence the dominance of this transport mechanism at the bottom part of aeolian dominated hillslopes.

In Cohen et al. (2015) we have also found that heterogeneity in soil distribution, derived from dominance of one of the two sediment transport mechanism, were considerably more pronounced in aeolian-dominated soilscapes. Generally, fluvial sediment transport in bedrock weathering dominated soilscapes, given enough time and pedoturbation stability, will lead to a source-limited flow regime which is in equilibrium with soil production rates (and thus soil depth; Cohen et al., 2015). This helps explain the patchy soil distribution in aeolian-dominated soilscapes and support our assertion in Cohen et al. (2015) that aeolian dominated soilscapes are more responsive (susceptible) to environmental changes.

Diffusion rate for this field site was found (based on an extensive parametric study) to have a weak and nonlinear relationship with topographic slope (β=0.1 in Eq. 4). This differs from the usual assumption of linearity (e.g. ref.) and may be due to the aeolian characteristics of the site's soilscape (fine PSD, absence of armouring mechanism, etc.) or may be attributed to the relatively steep and concave-down (increase in gradient downslope) characteristics of this field site. This will be the focus of a future study.

The overarching goal of this study is the investigation of the history of this region's soilscape evolution in the context of anthropogenically and climatologically driven soil depletion from hillslopes in Europe and southern Israel. The results demonstrate that soil distribution in our field site are highly susceptible to short environmental change. This is in contrast to the results of Cohen et al. (2013) which demonstrated that the response of bedrock weathering dominated soilscapes to climatic shifts will be a slow transition toward a new steady-state conditions. From this we can again conclude that aeolian dominated soilscapes are more susceptible to environmental change and thus even a relatively small change will lead to considerable alterations. The sharp increase in soil erodibility in the P3 stage representing anthropogenic activity have lead to the good agreement between our simulation results and the observed soil depth distribution at the field. This suggests that

Sagy Cohen 3/29/2016 10:21 AM
Deleted:

Sagy Cohen 3/29/2016 10:06 AM
Deleted: armored

Sagy Cohen 3/29/2016 10:24 AM
Formatted: Highlight

a) soil cover in our field site's hillslopes might have been more extensive during the early Holocene, and b) anthropogenic activity could have led to the soil-depleted hillslopes we observe today.

Soilscape evolution and distribution is typically calculated as a function of landscape topography (as was done here). However, we may also think of an opposite interaction, the effect of soil distribution on landscape evolution (i.e. topography) as studied by *Roering* (2008) on a soil-mantled landscape. The concave shape of the hillslope in this site may be linked to soil thickening downslope. Thicker soil in this soil-depleted landscape is likely to increase rock weathering (following the 'hump' weathering rate concept), which in this site (limestone dominated lithology) is mostly dissolution, leading to topographic lowering. This process is evident in the micro-topography along the hillslopes (likely propagated by soil/vegetation patches) and from *Saco et al*. (2007) which showed that soil/vegetation bands alter landscape morphology in water-limited environments. This suggests that the massive influx of aeolian sediment during the late-Pleistocene and early-Holocene may have considerably altered the morphology of this landscape, suggesting a strong coupling between soil production and landscape evolution, a hypothesis that needs to be further investigated.

5. Conclusions

Fluvial and diffusive sediment transport mechanisms lead to distinctively different soilscape evolutionary paths. Under erosive conditions - when transport rates are higher than sediment supply rates - the fluvial mechanism resulted in downslope thinning in soil depth while the diffusion led to downslope thickening. Neither mechanism was able to produce a soil distribution corresponding to that observed in our field-site. Only when both fluvial and diffusive sediment transport mechanisms were modeled, a reasonable correspondence was achieved. While soilscapes are generally thought off as resulting from both transport mechanisms, this and previous studies demonstrates that fluvial-diffusion coupling is more pronounced in aeolian dominated soilscape.

The results also point to soil distribution features that are indicative of the different sediment transport mechanism. It suggests that, for our semiarid aeolian-dominated field-site, diffusive transport is the dominant mechanism at the top part of the hillslope and fluvial processes are dominant at the. This is in contrast to bedrock weathering dominated soilscapes in which the opposite was observed as increased surface armouring downslope reduces fluvial transport.

Temporal variability in external drivers was shown to be a significant factor in this site's soilscape evolution. This demonstrates the importance of explicitly accounting for geomorphic processes and temporal variability in environmental and anthropogenic dynamics in order to understand the soilscape history, particularly in highly pedogenetic, anthropogenic and climatologically dynamic regions.

This study advanced our understanding of this region's soilscape evolution by elucidating the sediment transport mechanism that may have led to the soil distribution we observe today. The results suggest that relatively swift environmental changes in the late Holocene (i.e. anthropogenic activity) could have considerably changed the site's soil distribution from a soil-

mantled hillslopes (albeit with thin loess apron in many locations) to the soil-depleted hillslopes we observe today. Additional research is needed (and is ongoing) to better confine the rates and spatiotemporal dynamics of soil erosion and development in this site.

Acknowledgments

This research was supported by the Israel Science Foundation (ISF) (grant 1184/11). GRW was supported by an Australian Research Council Australian Professorial Fellowship.

References

Ahnert, F., (1977), Some comments on the quantitative formulation of geomorphological process in a theoretical model, *Earth Surface Processes*, 2, 191–201.

Almogi-Labin, A., M. Bar-Matthews, D. Shriki, E. Kolosovsky, M. Paterne, B. Schilman, A. Ayalon, Z. Aizenshtat, and A. Matthews (2009), Climatic variability during the last similar to 90 ka of the southern and northern Levantine Basin as evident from marine records and speleothems, *Quaternary Science Reviews*, *28*(25-26), 2882-2896.

Avni, Y., N. Porat, J. Plakht, and G. Avni (2006), Geomorphic changes leading to natural desertification versus anthropogenic land conservation in an and environment, the Negev Highlands, Israel, *Geomorphology*, *82*(3-4), 177-200.

Bowman, D., A. Karnieli, A. Issar, and H. J. Bruins (1986), Residual Colluvio-aeolian Aprons in the Negev Highlands (Israel) as a. Paleo-Climatic Indicator, *Palaeogeography Palaeoclimatology Palaeoecology*, 56(1-2), 89-101.

Bruins, H.J., and D.H. Yaalon (1992), Parallel advance of slopes in aeolian loess deposits of the northern Negev, Israel, *Israel Journal of Earth Sciences*, 41, 189–199.

Butzer, K. W. (2005), Environmental history in the Mediterranean world: cross-disciplinary investigation of cause-and-effect for degradation and soil erosion, *Journal of Archaeological Science*, 32(12), 1773-1800.

Carson, M. A., and M. J. Kirkby (1972), Hillslope Form and Process, 475 pp., Cambridge Univ. Press, Cambridge, U.K.

Cohen, S., G. Willgoose, and G. Hancock (2013), Soil–landscape response to mid and late Quaternary climate fluctuations based on numerical simulations, *Quaternary Research*, 79 (3): 452–457. doi: 10.1016/j.yqres.2013.01.001

Cohen, S., G. Willgoose, and G. Hancock (2010), The mARM3D spatially distributed soil evolution model: three-dimensional model framework, and analysis of hillslope and landform responses, *Journal of Geophysical Research-Earth Surface*, 115, F04013, doi:10.1029/2009JF001536.

Cohen, S., G. Willgoose, and G. Hancock (2009), The mARM spatially distributed soil evolution model: A computationally efficient modeling framework and analysis of hillslope soil surface organization, *Journal of Geophysical Research-Earth Surface*, 114, F03001, doi:10.1029/2008JF001214.

Sagy Cohen 3/22/2016 4:56 PM
Formatted: Font:10 pt

Sagy Cohen 3/22/2016 4:56 PM
Formatted: Font:10 pt

Cohen, S., G. Willgoose, T. Svoray, G. Hancock, and S. Sela (2015), The effects of sediment transport, weathering and aeolian mechanisms on soil evolution, *Journal of Geophysical Research-Earth Surface*, 120: 260–274. DOI: 10.1002/2014JF003186

Eldridge, D. J., E. Zaady, and M. Shachak (2002), Microphytic crusts, shrub patches and water harvesting in the Negev Desert: the Shikim system, *Landscape Ecology*, 17(6), 587-597.

Fleming R. W. and A. M. Johnson (1975), Rates of seasonal creep of silty clay soil, *Quarterly Journal of Engineering Geology*, 8: 1–29.

Fuchs, M. (2007), An assessment of human versus climatic impacts on Holocene soil erosion in NE Peloponnese, Greece, *Quaternary Research*, 67(3), 349-356.

Fuchs, M., A. Lang, and G. A. Wagner (2004), The history of Holocene soil erosion in the Phlious Basin, NE Peloponnese, Greece, based on optical dating, *Holocene*, 14(3), 334-345.

Gilbert, G.K., (1877), Report of the Henry Mountains (Utah), US Geographical and Geological Survey of Rocky Mountains Region, US Government Printing Office, Washington DC. 169pp.

Goodfriend, G. A. (1987), Chronostratigraphic studies of sediments in the Negev desert, using amino acid epimerization analysis of land snail shells, *Quaternary Research*, 28(3), 374-392.

Hancock G R, G R Willgoose K G Evans, 2002. Testing of the SIBERIA landscape evolution model using the Tin Camp Creek, Northern Territory, Australia, field catchment, *Earth Surface Processes and Landforms*, 27, 125-143.

Heimsath, A.M., Chappell, J.C., Spooner, N.A., Questiaux, D.G., (2002), Creeping soil. *Geology*. 30(2): 111-114.

Heimsath, A. M., Dietrich, W. E., Nishiizumi, K., and Finkel R. C., (1997), The soil production function and landscape equilibrium, *Nature*, 388(6640), 358-361.

Horowitz, A., (1979), The Quaternary of Israel: New York, Academic Press, 394 p.

Hughes, M. W., Almond, P.C., Roering, J. J., and Tonkin, P. J., (2010), Late Quaternary loess landscape evolution on an active tectonic margin, Charwell Basin, South Island, New Zealand, *Geomorphology*, 122, 294-308.

Hughes, M. W., Schmidt, J., and Almond, P.C., (2009), Automatic landform stratification and environmental correlation for modeling loess landscape in North Otago, South Island, New Zealand, *Geoderma*, 149, 92-100.

Istanbulluoglu, E., D. Tarboton, R. Pack, and C. Luce (2004), Modeling of the interactions between forest vegetation, disturbances, and sediment yields, *J. Geophys. Res. -Earth Surf., 109*(F1), F01009, doi: 10.1029/2003JF000041.

Kim, J., and V. Y. Ivanov (2014), On the nonuniqueness of sediment yield at the catchment scale: The effects of soil antecedent conditions and surface shield, Water Resour. Res., 50(2), 1025–1045, doi:10.1002/2013WR014580.

Langbein, W.B. and Schumm, S.A., (1958), Yield of sediment in relation to mean annual precipitation, *Transactions of the American Geophysical Union*, 39, 1076-1084.

Ludwig, J., B. Wilcox, D. Breshears, D. Tongway, and A. Imeson (2005), Vegetation patches and runoff-erosion as interacting ecohydrological processes in semiarid landscapes, Ecology, 86(2), 288-297, doi: 10.1890/03-0569.

Sagy Cohen 3/22/2016 4:56 PM
Formatted: Font:10 pt

Sagy Cohen 3/22/2016 10:23 AM
Deleted: Engelhund, F., and E. Hansen (1968), A Monograph on Sediment Transport in Alluvial Streams. Teknish Forlag, Technical Press, Copenhagen, Denmark 62 pp.

Sagy Cohen 3/22/2016 4:56 PM
Formatted: Font:10 pt

McFadden, L.D. and P.L.K. Knuepfer (1990), Soil geomorphology: the linkage of pedology and superficial processes ,in: P.L.K. Knuepfer, L.D. MacFadden (Eds.), Soils and Landscape Evolution, *Geomorphology*, 3, 197–205.

Minasny, B., and McBratney, A.B. (2006), Mechanistic soil-landscape modelling as an approach to developing pedogenesis classifications. *Geoderma*, 133: 138-149.

Neave, M. and S. Rayburg (2007), A field investigation into the effects of progressive rainfall-induced soil seal and crust development on runoff and erosion rates: The impact of surface cover, *Geomorphology, 87*(4), 378-390.

Roering, J. J. (2004), Soil creep and convex-upward velocity profiles: Theoretical and experimental investigation of disturbance-driven sediment transport on hillslopes, *Earth Surface Processes and Landforms*, 29(13), 1597-1612.

Roering, J. J. (2008), How well can hillslope evolution models "explain" topography? Simulating soil transport and production with high-resolution topographic data, *Geological Society of America Bulletin*, 120(9-10), 1248-1262.

Saco, P. M., Willgoose, G.R., and Hancock, G. R., (2007) Eco-geomorphology of banded vegetation patterns in arid and semi-arid regions, *Hydrology and Earth System Sciences*, 11, 1717-1730.

Sela, S., T. Svoray, and S. Assouline (2012), Soil water content variability at the hillslope scale: Impact of surface sealing, *Water Resources Research,* 48, W03522, doi: 10.1029/2011WR011297.

Sommer, M., H. H. Gerke, and D. Deumlich (2008), Modelling soil landscape genesis - A "time split" approach for hummocky agricultural landscapes, *Geoderma*, 145(3-4), 480-493.

Svoray, T., Karnieli A. 2011. Rainfall, topography, and primary production relationships in a semiarid ecosystem. *Ecohydrology*, 4, 56-66.

Svoray, T., R. Shafran-Nathan, Z. Henkin, and A. Perevolotsky (2008), Spatially and temporally explicit modeling of conditions for primary production of annuals in dry environments, *Ecological Modelling*, *218*(3-4), 339-353.

Tarboton, D., G. (1997), A New Method for the Determination of Flow Directions and Contributing Areas in Grid Digital Elevation Models. *Water Resources Research*, 33(2), 309-319.

Tarboton, D., G. (2010) Terrain Analysis Using Digital Elevation Models (TauDEM), Utah State University Logan, available at: http://hydrology.neng.usu.edu/taudem

TOPOG (1997): http://www-data.wron.csiro.au/topog/user/user.html

Tucker, G. E., and G. R. Hancock (2010), Modelling landscape evolution, *Earth Surface Processes and Landforms*, 35(1), 28-50.

Vaks, A., M. Bar-Matthews, A. Ayalon, B. Schilman, M. Gilmour, C. J. Hawkesworth, A. Frumkin, A. Kaufman, and A. Matthews (2003), Paleoclimate reconstruction based on the timing of speleothem growth and oxygen and carbon isotope composition in a cave located in the rain shadow in Israel, *Quaternary Research*, 59(2), 182-193.

Vaks, A., M. Bar-Matthews, A. Ayalon, A. Matthews, A. Frumkin, U. Dayan, L. Halicz, A. Almogi-Labin, and B. Schilman (2006), Paleoclimate and location of the border between Mediterranean climate region and the Saharo-Arabian Desert as revealed by speleothems from the northern Negev Desert, Israel, *Earth and Planetary Science Letters*, 249(3-4), 384-399.

Sagy Cohen 3/22/2016 4:56 PM
Formatted: Font:10 pt

Sagy Cohen 3/22/2016 5:54 PM
Formatted: Normal, Indent: Left: 0", Hanging: 0.31"

Sagy Cohen 3/22/2016 4:56 PM
Formatted: Font:10 pt

Sagy Cohen 3/22/2016 4:56 PM
Formatted: Font:10 pt

Unknown
Field Code Changed

Sagy Cohen 3/22/2016 4:56 PM
Formatted: Font:10 pt

van Andel, T. H., E. Zangger, and A. Demitrack (1990), Land use and soil erosion in prehistoric and historic Greece , *Journal of Field Archaeology*, 17(4), 379-396.

Wells, T., Willgoose G. and G Hancock G (2008), Modelling weathering pathways and processes of the fragmentation of salt weathered quartz-chlorite schist, *Journal of Geophysical Research- Earth Surface*, 113, F01014.

Willgoose, G. R., and Sharmeen, S., (2006), A One-dimensional model for simulating armouring and erosion on hillslopes: I. Model development and event-scale dynamics, *Earth Surface Processes and Landforms*, 31, 970-991.

Yair, A., and A. Kossovsky (2002), Climate and surface properties: hydrological response of small and and semi-arid watersheds, *Geomorphology*, 42(1-2), 43-57.

Yoo, K., and S. M. Mudd (2008), Discrepancy between mineral residence time and soil age: Implications for the interpretation of chemical weathering rates, *Geology*, 36(1), 35–38.

Zilberman, E. (1992), The late Pleistocene sequence of the northwestern Negev flood plains — a key to reconstructing the paleoclimate of southern Israel in the last glacial, *Isr. J. Earth-Sci.* 41, 155–167.

Table and Figure captions

Table 1. Values of the parameters that are driven by the simulation scenario. P1, P2 and P3 are the three simulated periods (80-12, 12-8 and 8-0 kyr BP respectively; Figure 3) and S1, S2 and S3 are the three simulation (Fluvial, Diffusive and Combined respectively).

	i: Erodibility, e (unitless; Eq. 1)	*ii*: Runoff, Q (m^3/y; Eq. 2)	*iii*: Aeolian deposition, K_a (mm/y; Eq. 5)	*iv*: Diffusive rate, D_s (mm/y; Eq. 3-4)
P1	S1: 0.0001 S2: 0.0 S3: 0.0001	S1: 0.0017 S2: 0.0 S3: 0.00066	S1: 0.1 S2: 0.1 S3: 0.1	S1: 0.0 S2: 21.5 S3: 12.0
P2	S1: 0.0002 S2: 0.0 S3: 0.0002	S1: 0.0034 S2: 0.0 S3: 0.00132	S1: 0.05 S2: 0.05 S3: 0.05	S1: 0.0 S2: 21.5 S3: 12.0
P3	S1: 0.001 S2: 0.0 S3: 0.001	S1: 0.017 S2: 0.0 S3: 0.0066	S1: 0.01 S2: 0.01 S3: 0.01	S1: 0.0 S2: 10.75 S3: 6.0

Figure 1. The study region and site. The Long Term Ecological Research, LTER, in southern Israel, is uniquely situated at a margin between Mediterranean climatic regime to the north and arid climate to the south (a). The study site is located on a Loess belt (b) deposited during the late-Pleistocene and early-Holocene. Hillslopes in this region are today mostly depleted of their Loess cover (c and d). The contour lines in (c) are at 2 m intervals.

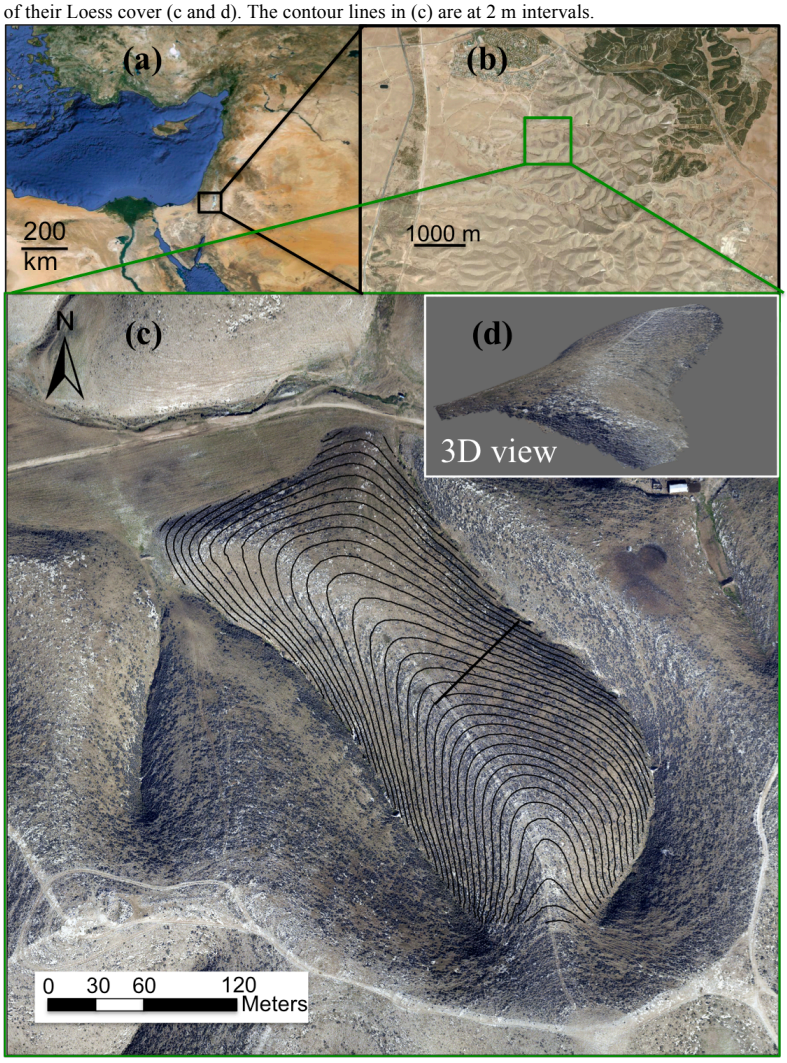

Figure 2. Soil depth at the Lehavim LTER site, measured in 350 locations and interpolated using Kriging. Pixels classified as rock from a 10 cm^2 orthophoto were assigned zero depth. The contour lines are at 2 m intervals and the thick black line is the location of the transect analyzed in section 3.3.

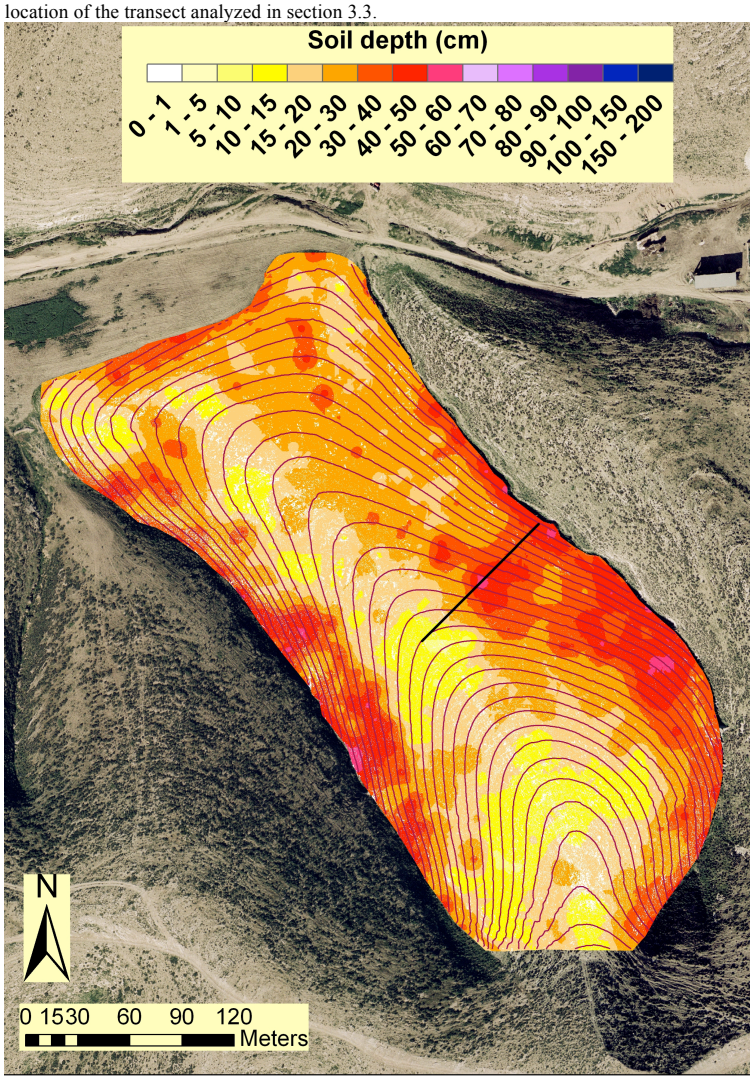

Figure 3. The simulation scenario. Describe the temporal changes in four model parameters as a function of climatic and anthropogenic drivers. The Erosion factor is overlapping with the Runoff generation line.

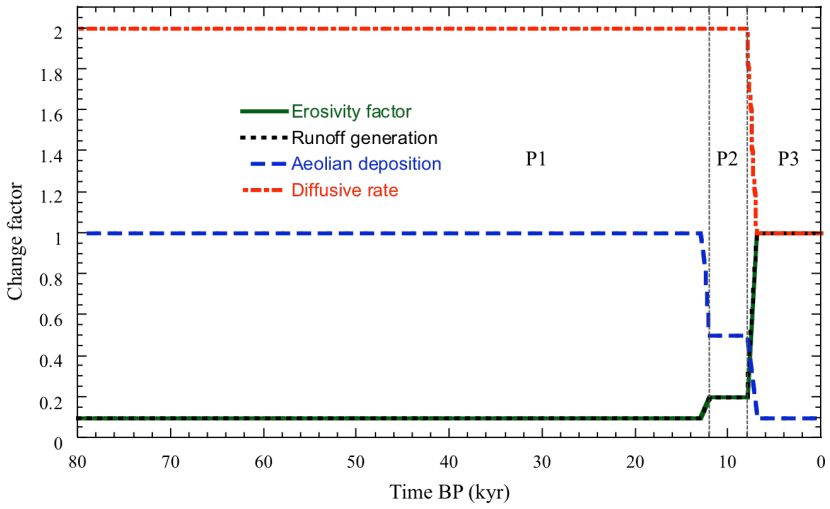

5

Figure 4. Soil depth maps produced by the Fluvial only simulation (S1) at 3.2 kyr time intervals in the last 18 of 80 kyr simulated: (a) 18 kyr BP (b) 12.8 kyr BP (end of P1); (c) 9.6 kyr BP; (d) 6.4 kyr BP (end of P2); (e) 3.2 kyr BP; and (f) 0 kyr BP (final/modern- end of P3). The contour lines represent 2 m change in topography.

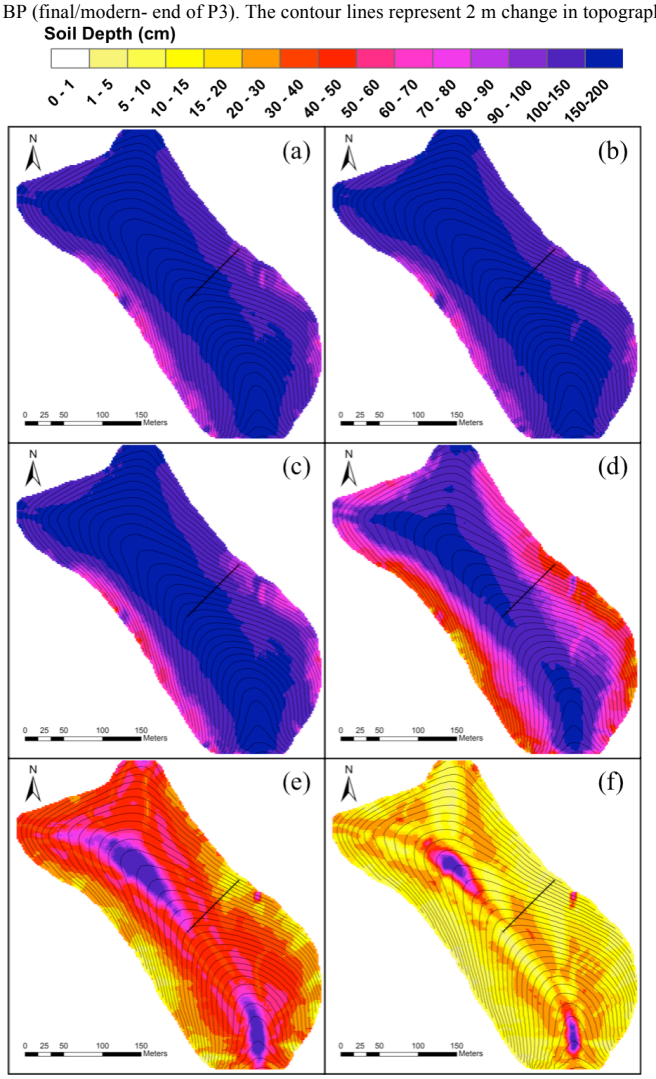

Figure 5. Soil depth maps produced by the Diffusive only simulation (S2) at 3.2 kyr time intervals in the last 18 of 80 kyr simulated: (a) 18 kyr BP (b) 12.8 kyr BP (end of P1); (c) 9.6 kyr BP; (d) 6.4 kyr BP (end of P2); (e) 3.2 kyr BP; and (f) 0 kyr BP (final/modern- end of P3). The contour lines represent 2 m change in topography.

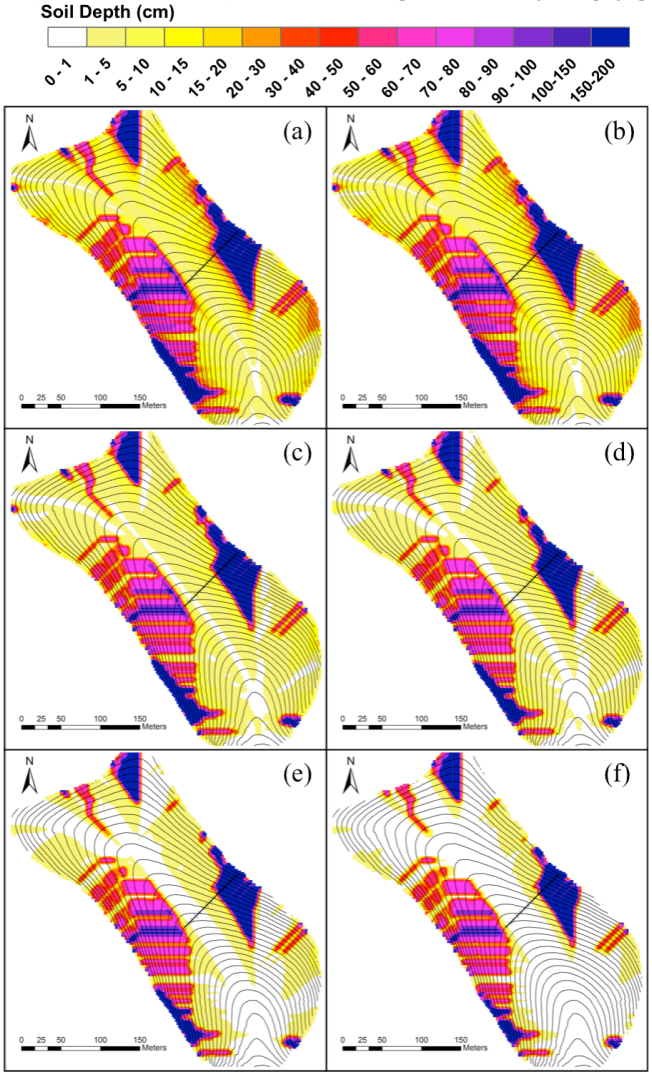

Figure 6. Soil depth maps produced by the Combined simulation (S3) at 3.2 kyr time intervals in the last 18 of 80 kyr simulated: (a) 18 kyr BP (b) 12.8 kyr BP (end of P1); (c) 9.6 kyr BP; (d) 6.4 kyr BP (end of P2); (e) 3.2 kyr BP; and (f) 0 kyr BP (final/modern- end of P3). The contour lines represent 2 m change in topography.

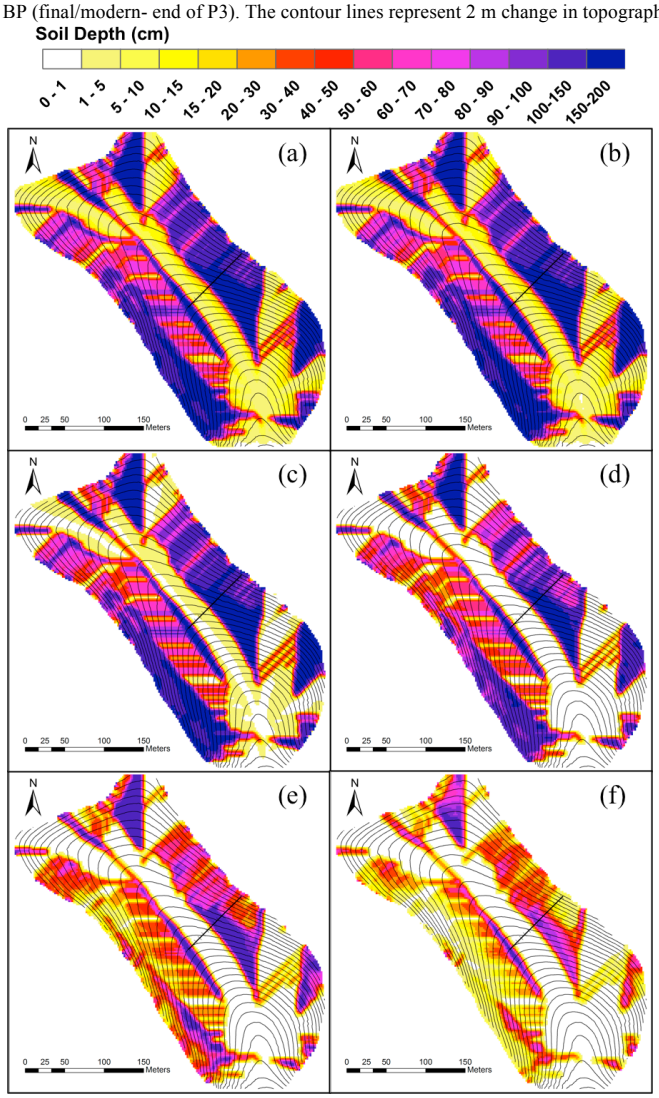

Figure 7. Soil depth across a transect (Figure 1c) on the northeastern facing hillslope at 6 time intervals (corresponding to soil maps in Figures 4-6): (a) the Fluvial only simulation (S1), (b) the Diffusive only simulation (S2), (c) the Combined simulation (S3), and (d) measured soil depth (Figure 2).

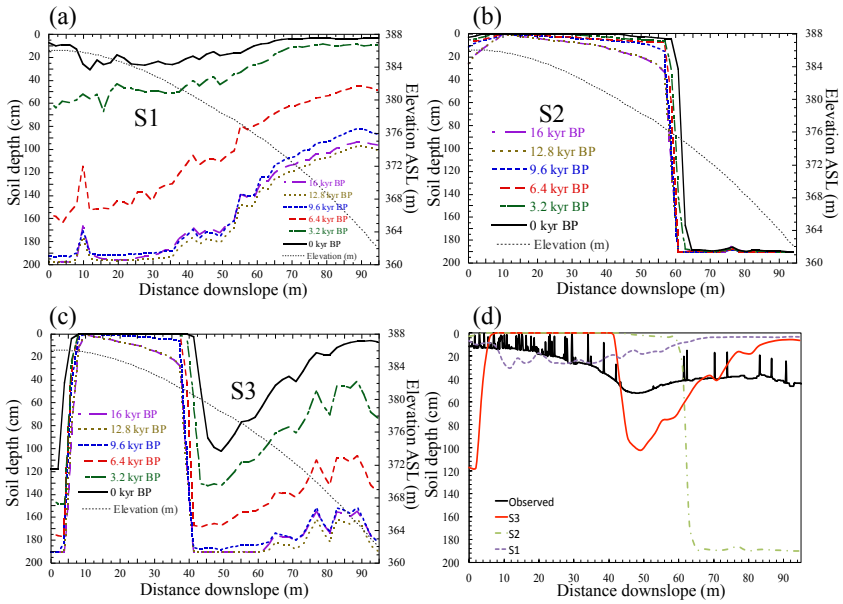

5